BJRS
BRAZILIAN JOURNAL OF RADIATION SCIENCES

doi.org/10.15392/2319-0612.2024.2455
2024, 12(3) | 01-23 | e2455
Submitted: 2024-03-14
Accepted: 2024-08-05

Analysis of the relationship between field size and change in radiation dose to patient and staff based on radiographic technique in fluoroscopy and radiography

Ferreira [a,b], K. C.; Denyak [a,c*], V.; Nunes [b], M. C. A.; Nunes [b], G.S.; Real [b], G. V.; Filipov [a], D.

[a] Federal University of Technology – Paraná, CEP 80230-901, Curitiba, Paraná, Brasil
[b] Brazilian Hospital Services Company, EBSERH - branch CHC-UFPR, CEP 80060-900, Curitiba, Paraná, Brasil
[c] National Science Center 'Kharkov Institute of Physics and Technology', 61108, Kharkiv, Ukraine

*Correspondence: denyak@gmail.com

Astract: In discussions of radiological protection issues in fluoroscopy and radiography the radiation field size is usually mentioned in connection with unnecessary irradiation of the patient's body parts that do not need to be imaged. However, excessive expansion of the field size leads also to some other effects: the excessive irradiation of assistants and visualized part of patient's body as well as the change in dose rate at the entrance of patient's body by automatic brightness control. The aim of the present paper is to describe the results of an experimental study of the dependence of such effects on irradiation field size and primary X-ray spectrum. The measurements were carried out in conditions close to those of barium meal test. To simulate the patient body, 5 acrylic plates measuring 30 cm high x 30 cm long x 3 cm thick each were used, totalling 15 cm thick. The X2 RF Sensor (RAYSAFE) was used to measure the dose rate at the entrance and exit surface of the simulator and the specific model for measuring leakage and dispersion, the X2 Survey sensor (RAYSAFE), was used to measure the occupational dose rate. The occupational dose rate detector was located at the position that assistant usually maintains to support the patient's head and/or to administer the contrast. The results show that in radiographic mode dose rate at the exit of the patient's body increases with the increase of field size. This increase reaches 85%. The increase of occupational dose rate in radiographic mode reaches 850% and is linearly proportional to the field area. In fluoroscopic mode, dose rate at the entrance of the patient's body decreases proportionally to the increase of field side length because of the automatic brightness control. This effect reaches 25% with grid and 50% without grid.

Keywords: fluoroscopy, radiography, radiation dose, field size.

BJRS
BRAZILIAN JOURNAL OF RADIATION SCIENCES

doi.org/10.15392/2319-0612.2024.2455
2024, 12(3) | 01-23 | e2455
Submitted: 2024-03-14
Accepted: 2024-08-05

Análise da relação entre tamanho do campo e alteração na dose de radiação no paciente e equipe baseada na técnica radiográfica em fluoroscopia e radiografia

Resumo: Nas discussões sobre questões de proteção radiológica em fluoroscopia e radiografia, o tamanho do campo de radiação é geralmente mencionado em conexão com a irradiação desnecessária de partes do corpo do paciente que não precisam ser visualizadas. Contudo, a expansão excessiva do tamanho do campo leva também a alguns outros efeitos: a irradiação excessiva de auxiliares e parte visualizada do corpo do paciente bem como a alteração da taxa de dose na entrada do corpo do paciente por controle automático de brilho. O objetivo do presente artigo é descrever os resultados de um estudo experimental da dependência de tais efeitos do tamanho do campo de irradiação e do espectro primário de raios X. As medições foram realizadas em condições próximas às da seriografia (SEED). Para simular o corpo do paciente foram utilizadas 5 placas de acrílico medindo 30 cm de altura x 30 cm de comprimento x 3 cm de espessura cada, totalizando 15 cm de espessura. O Sensor RF X2 (RAYSAFE) foi utilizado para medir a taxa de dose na superfície de entrada e saída do simulador e o modelo específico para medição de vazamento e dispersão, o sensor X2 Survey (RAYSAFE), foi utilizado para medir a taxa de dose ocupacional. O detector de taxa de dose ocupacional foi localizado na posição que o auxiliar costuma manter para apoiar a cabeça do paciente e/ou para administrar o contraste. Os resultados mostram que no modo radiográfico a taxa de dose na saída do corpo do paciente aumenta com o aumento do tamanho do campo. Esse aumento chega a 85%. O aumento da taxa de dose ocupacional no modo radiográfico chega a 850% e é linearmente proporcional à área do campo. No modo fluoroscópico, a taxa de dose na entrada do corpo do paciente diminui proporcionalmente ao aumento do tamanho do campo devido ao controle automático de brilho. Este efeito chega a 25% com grade e 50% sem grade.

Palavras-chave: fluoroscopia, radiografia, dose de radiação, tamanho do campo.

SBPR

1. INTRODUCTION

Fluoroscopy is used in a wide variety of medical examinations and procedures to evaluate, in real time, the anatomy, physiology and possible pathologies of internal organs or treat patients. It employs ionizing radiation and implies radiation exposure of patients and staff with doses that can be rather high. Due to the importance of this issue many documents of various international organizations discuss guidelines for optimization and radiological protection in fluoroscopy [1-7]. The inadvertent irradiation of the medical staff performing this procedure in examination room is another concern. It is possible to reduce the dose values optimizing various technical parameters of fluoroscopic equipment.

One of such parameters is the radiation field size. This parameter is usually discussed in connection with unnecessary irradiation of the patient's body parts that do not need to be imaged [8]. However, excessive expansion of the field size leads also to some other effects:

- Fluoroscopic examinations are usually accompanied by production of various radiographic images. In radiographic mode, the unnecessary irradiated patient's body parts turn into new sources of scattered radiation, which degrades image quality and irradiates assistants who remain inside the examination room during the procedure.
- In fluoroscopic mode, the automatic brightness control changes the dose rate at the entrance of the patient's body. Even modern detectors used in automatic brightness control are not capable of evaluating the intensity of radiation in this or that part of the image. They assess the total intensity of radiation passing through the patient and this intensity increases proportionally to the irradiated area. To maintain the same brightness (same intensity of radiation passing through the patient) the equipment has to change the dose rate at the entrance.

This work continues our research into the influence of various technical parameters of fluoroscopic equipment on patient and occupational dose begun earlier [9,10]. In the present work, our goals were to analyse how the mention above effects depend on irradiation field size and primary X-ray spectrum. First, we studied the change in dose rate at the exit of the patient's body and in occupational dose rate in radiographic mode. Then, we investigated the change in dose rate at the entrance of the patient's body and in occupational dose rate in fluoroscopic mode.

2. MATERIALS AND METHODS

The study was carried out in a University Hospital in the city of Curitiba (Brazil), in the Department of Radiology, in January 2023. The research was not submitted to the Institutional Review Board for not involving human beings.

The fluoroscopy equipment used was the remote-controlled system AXIOM ICONOS MD, Siemens, 2006 A detailed description of the equipment can be found in Nunes et al [9].

To measure the dose rate of ionizing radiation, RAYSAFE solid-state detectors were used together with a Base X2 unit to read the results [11]. The X2 RF Sensor was used to measure the dose rate at the entrance and exit surface of the simulator and the specific model for measuring dispersion, the X2 Survey sensor, was used to measure the occupational dose rate. The calibration certificates for the both detectors were issued by the Unfors Raysafe AB Laboratory on 22 June 2022.

To simulate the patient body, 5 acrylic plates measuring 30 cm high x 30 cm long x 3 cm thick each were used, totalling 15 cm thick. This thickness was adopted considering, for example, skull of a typical adult patient [12] or thorax of a ~10-year-old paediatric patient from the same hospital [13].

The measurements were carried out in conditions close to those of barium meal test routinely performed in this hospital. Fig. 1 and 2 shows the experimental setup. The center of the X-ray beam was positioned exactly at the center of the patient simulator. The focus of the X-ray tube and the center of the patient simulator were located at 102 cm from the floor. The table was arranged vertically and the patient simulator was positioned on a support against the examination table with a horizontal distance of 90 cm from the focus of the X-ray tube. The image intensifier was at 115 cm from the focus. The detectors at the entrance and exit of the simulator were positioned at the center of the irradiation field.

Figure 1: Experimental setup. 1) X-ray tube. 2) Patient simulator. 3) Detector at the exit of the patient simulator. 4) Occupational dose detector. 5) Detector at the entrance of the simulator. 6) Table. 7) Image Intensifier.

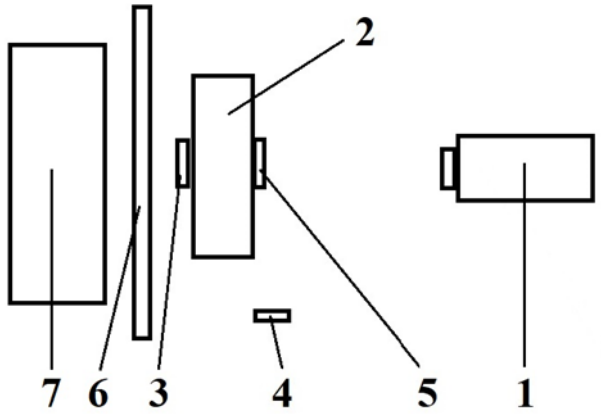

Figure 2: Experimental setup. 1) X-ray tube. 2) Patient simulator. 4) Occupational dose detector.

The occupational dose rate detector was located on the lead apron positioned at 50 cm from the center of the patient simulator, representing the position that assistant usually maintains to support the patient's head and/or to administer the contrast. In the vertical direction, the detector was positioned in three ways to measure dose rates on the face (its center was 140 cm from the floor), thorax (110 cm from the floor) and pelvis (80 cm from the floor).

In radiographic mode, the dose rate measurements were performed for different kVp, filters and field sizes (Table 1). In fluoroscopic mode, the kVp values were automatically chosen by the equipment.

Table 1: Technical parameters

	Radiographic mode	**Fluoroscopic mode**
Field size on the table, cm^2	10 x 10 16 x 16 22 x 22 28 x 28	10 x 10 12 x 12 16 x 16 20 x 20 22 x 22 28 x 28
Additional filtration (mmCu)	Without 0.1 0.2 0.3	Without 0.1 0.2 0.3
Grid	Yes	Yes No
kVp	70 81 90 100	Automatically

To estimate the statistic errors, three dose rate measurements were performed for each adopted parameter, totalling 1272 tests. We analysed the increase factor of the dose rate: the ratio between the dose rate for a particular field size and for the smallest one.

3. RESULTS AND DISCUSSIONS

3.1. Change in dose rate at the exit of the patient's body in radiographic mode

The mean values and standard deviations of the increase factor of the exit dose rate are presented in Table 2 as a function of kVp, field size and filter thickness. The exit dose rates were normalized with respect to the entrance dose rate.

Table 2: Mean values and standard deviations of the increase factor of the exit dose rate as a function of kVp, field size and filter thickness (radiographic mode).

Field size (cm^2)	kVp			
	70	**81**	**90**	**100**
Filter of 0.3 mm				
28 x 28	1.86±0.06	1.86±0.04	1.88±0.02	1.86±0.03
22 x 22	1.70±0.04	1.69±0.03	1.69±0.04	1.69±0.03
16 x 16	1.36±0.05	1.36±0.04	1.36±0.04	1.35±0.05
10 x 10	1.00±0.03	1.00±0.04	1.00±0.03	1.00±0.03
Filter of 0.2 mm				
28 x 28	1.84±0.06	1.85±0.03	1.86±0.02	1.86±0.03
22 x 22	1.69±0.03	1.69±0.02	1.69±0.03	1.70±0.02
16 x 16	1.36±0.05	1.36±0.05	1.35±0.04	1.35±0.04
10 x 10	1.00±0.04	1.00±0.04	1.00±0.04	1.00±0.03
Filter of 0.1 mm				
28 x 28	1.83±0.03	1.83±0.03	1.84±0.03	1.84±0.03
22 x 22	1.68±0.03	1.67±0.03	1.67±0.04	1.69±0.03
16 x 16	1.35±0.05	1.36±0.05	1.35±0.04	1.34±0.04
10 x 10	1.00±0.03	1.00±0.04	1.00±0.03	1.00±0.03
Without filter				
28 x 28	1.78±0.05	1.79±0.04	1.82±0.03	1.83±0.03
22 x 22	1.66±0.02	1.66±0.04	1.66±0.04	1.68±0.03
16 x 16	1.35±0.05	1.34±0.04	1.34±0.04	1.34±0.04
10 x 10	1.00±0.03	1.00±0.04	1.00±0.03	1.00±0.03

The increase reaches 85% and does not depend on either the kVp or the filter thickness, that is, the primary X-ray spectrum. Possible difference between increase factors does not exceed 4% which matches the accuracy of the detector.

Fig. 3 shows the increase factors for the two opposite situations: the primary X-ray spectra of highest and lowest average energies. The primary X-ray spectrum for 70 kVp without filter has the lowest average energy and the spectrum for 100 kVp and the filter thickness of 0.3 mm has the highest average energy. The other spectra gave the results between these two. The lines and formulas in Fig. 3 are the results of fitting of a second-order polynomial to the results of all measurements. This formula allows evaluating the increase factors in relation to the 10 cm field. It can be rewritten for any field as a reference point. For that, it is necessary to calculate the value of the increase factors for the new reference point using this formula and then divide the coefficients in it by a value equal to this increase factor.

Figure 3: Increase factor (D/D_{10}) of the exit dose rate as a function of field side length (L) and area (S) (radiographic mode).

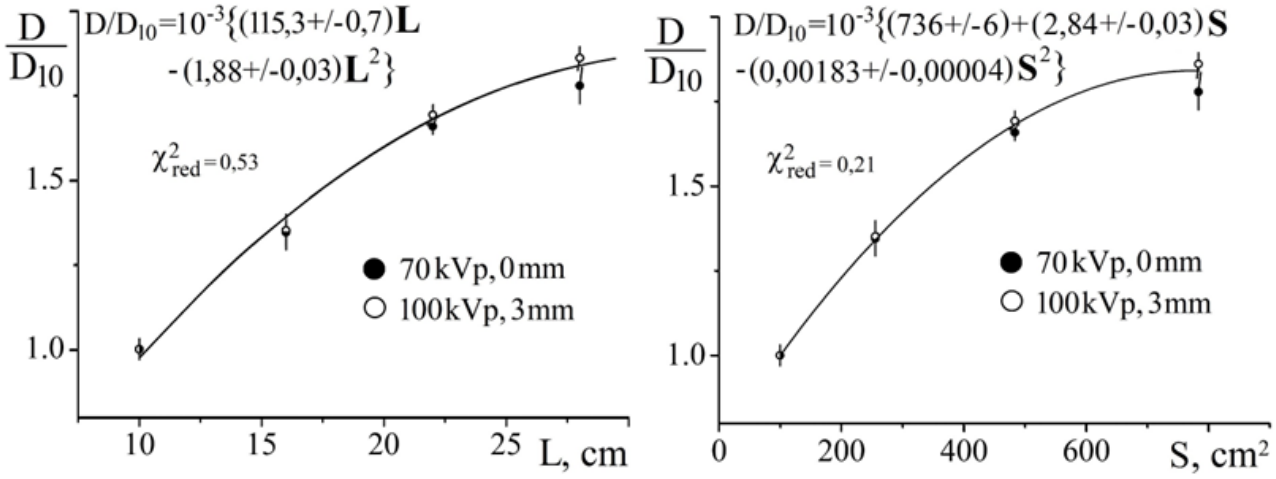

The number of scattering points that contribute to the increase factor is linearly proportional to the field area, but the dose rate increases more slowly. The explanation for this effect lies in absorption of the scattered photons (a) and in increasing of the scattering angle in relation to the direction of the primary beam (b):

a) As the area increases, the distance between the center of the field and the scattering point increases. The scattered photon has to travel a greater distance to reach the detector in the center of the field. This means that the probability of this photon being absorbed by the acrylic also increases.

b) As the scattering point moves away from the field center, the scattering angle increases in relation to the direction of the primary beam (angle θ in Fig. 4). The scattering probability is very sensitive to this angle and decreases rapidly with its increase.

Figure 4: Scattering angle.

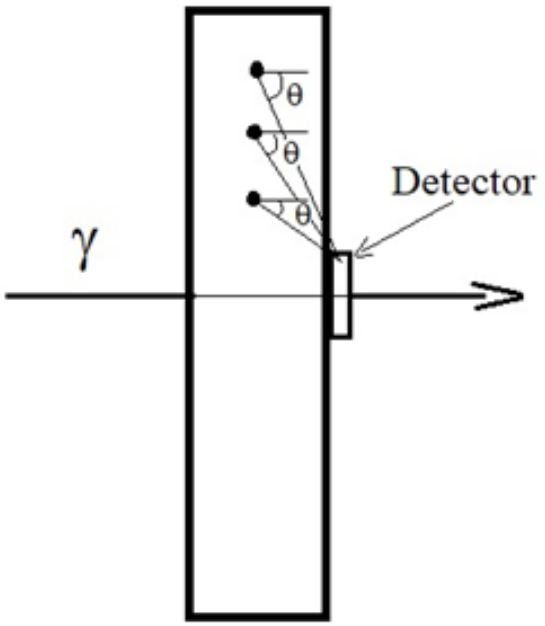

Increase of the dose rate at the exit of the patient's body is important not only because of unnecessary exposure of the patient. It also influences the image quality. All photons increasing the dose rate are the scattered photons i.e., they came from another parts of the body, thus worsening the image quality.

3.2. Change in occupational dose rate in radiographic mode

The increase factors of the dose rate in the various regions of the professional's body are shown in Tables 3-5 as a function of kVp, field size and filter thickness. The dose rates were normalized with respect to the entrance dose rate.

Table 3: Mean values and standard deviations of the increase factors of the dose rate in the facial region as a function of kVp, field size and filter thickness (radiographic mode).

Field size (cm^2)	kVp			
	70	**81**	**90**	**100**
Filter of 0.3 mm				
28 x 28	8.80±0,20	8.40±0.17	8.17±0.19	8.14±0.14
22 x 22	5.38±0,27	5.17±0.23	5.07±0.25	4.98±0.24
16 x 16	2.72±0,12	2.64±0.11	2.63±0.12	2.59±0.13
10 x 10	1.00±0,09	1.00±0.05	1.00±0.06	1.00±0.06
Filter of 0.2 mm				
28 x 28	8.53±0.21	8.14±0.20	8.17±0.18	8.12±0.15
22 x 22	5.25±0.30	5.04±0.23	5.06±0.24	5.00±0.26
16 x 16	2.68±0.15	2.59±0.10	2.61±0.10	2.58±0.09
10 x 10	1.00±0.09	1.00±0.07	1.00±0.06	1.00±0.06
Filter of 0.1 mm				
28 x 28	8.30±0.16	8.28±0.14	8.17±0.14	8.10±0.15
22 x 22	5.09±0.24	5.06±0.28	5.03±0.24	5.01±0.20
16 x 16	2.58±1.10	2.61±0.12	2.59±0.10	2.57±0.10
10 x 10	1.00±0.07	1.00±0.07	1.00±0.07	1.00±0.07
Without filter				
28 x 28	8.18±0.22	8.17±0.19	8.08±0.17	8.10±0.19
22 x 22	5.02±0.28	5.05±0.26	4.95±0.25	5.02±0.21
16 x 16	2.58±0.12	2.57±0.11	2.56±0.12	2.59±0.10
10 x 10	1.00±0.06	1.00±0.07	1.00±0.07	1.00±0.07

Table 4: Mean values and standard deviations of the increase factors of the dose rate in the thorax region as a function of kVp, field size and filter thickness (radiographic mode).

Field size (cm^2)	kVp			
	70	**81**	**90**	**100**
Filter of 0.3 mm				
28 x 28	8.65±0.25	8.41±0.18	8.32±0.29	8.26±0.22
22 x 22	5.34±0.26	5.22±0.16	5.16±0.16	5.10±0.19
16 x 16	2.73±0.10	2.68±0.10	2.67±0.10	2.65±0.12
10 x 10	1.00±0.04	1.00±0.05	1.00±0.05	1.00±0.04
Filter of 0.2 mm				
28 x 28	8.44±0.16	8.47±0.24	8.33±0.26	8.24±0.25
22 x 22	5.24±0.17	5.25±0.21	5.13±0.15	5.10±0.14
16 x 16	2.68±0.10	2.69±0.16	2.64±0.14	2.64±0.11
10 x 10	1.00±0.04	1.00±0.04	1.00±0.05	1.00±0.04
Filter of 0.1 mm				
28 x 28	8.47±0.24	8.51±0.38	8.37±0.22	8.31±0.31
22 x 22	5.19±0.25	5.25±0.20	5.19±0.18	5.17±0.18
16 x 16	2.63±0.15	2.67±0.13	2.67±0.10	2.66±0.10
10 x 10	1.00±0.04	1.00±0.03	1.00±0.05	1.00±0.04
Without filter				
28 x 28	8.57±0.22	8.37±0.20	8.37±0.13	8.36±0.18
22 x 22	5.20±0.21	5.17±0.17	5.16±0.21	5.23±0.18
16 x 16	2.66±0.13	2.65±0.09	2.67±0.11	2.66±0.11
10 x 10	1.00±0.05	1.00±0.05	1.00±0.05	1.00±0.03

Table 5: Mean values and standard deviations of the increase factors of the dose rate in the pelvic region as a function of kVp, field size and filter thickness (radiographic mode).

Field size (cm^2)	kVp			
	70	**81**	**90**	**100**
Filter of 0.3 mm				
28 x 28	7.86±0.09	7.65±0.21	7.55±0.14	7.42±0.14
22 x 22	5.03±0.10	4.97±0.06	4.89±0.03	4.77±0.07
16 x 16	2.65±0.08	2.61±0.08	2.60±0.08	2.56±0.08
10 x 10	1.00±0.02	1.00±0.02	1.00±0.02	1.00±0.02
Filter of 0.2 mm				
28 x 28	7.73±0.08	7.55±0.17	7.50±0.20	7.43±0.12
22 x 22	4.98±0.03	4.82±0.03	4.85±0.03	4.79±0.04
16 x 16	2.66±0.09	2.58±0.09	2.61±0.09	2.56±0.09
10 x 10	1.00±0.02	1.00±0.01	1.00±0.02	1.00±0.01
Filter of 0.1 mm				
28 x 28	7.59±0.09	7.57±0.10	7.57±0.12	7.49±0.13
22 x 22	4.90±0.07	4.87±0.03	4.85±0.03	4.86±0.11
16 x 16	2.61±0.07	2.62±0.08	2.58±0.07	2.60±0.08
10 x 10	1.00±0.02	1.00±0.02	1.00±0.02	1.00±0.01
Without filter				
28 x 28	7.60±0.12	7.45±0.22	7.51±0.24	7.44±0.13
22 x 22	4.88±0.05	4.85±0.06	4.82±0.08	4.84±0.05
16 x 16	2.62±0.11	2.57±0.10	2.60±0.08	2.57±0.08
10 x 10	1.00±0.01	1.00±0.01	1.00±0.01	1.00±0.02

The increase of the dose rate is significant and may be greater than 850%. There are signs of an increase in this factor with a decrease in kVp and an increase in the thickness of the filter. But this effect does not exceed 10% and was statistically confirmed only for some kVp and filter thicknesses in the face and pelvic regions.

Analysing the dependence on kVp, the statistically significant differences were observed:

1. In the facial region only for field size 28 x 28 cm^2 and filter thickness of 0.3 mm between 70 and 90 or 70 and 100 kVp;

2. In the pelvic region, for field size 28 x 28 cm^2 and filter thicknesses of 0.3 and 0.2 mm between 70 and 100 kVp;

3. In the pelvic region, for field size 22 x 22 cm^2 and filter thicknesses of 0.3 mm between 70 and 100 kVp or 81 and 100 kVp.

All these differences are more than two but less than three errors and cannot be considered statistically detected. The only differences that exceed three errors are observed in the pelvic region for field size 22 x 22 cm^2 and filter thicknesses of 0.2 mm between 70 and 81 or 90 or 100 kVp.

Considering the dependence on filter thickness, all observed differences greater than two errors do not exceed three errors:

1. In the facial region, for field size 28 x 28 cm^2 and 70 kVp between filter thicknesses of 0.3 and 0 mm;

2. In the pelvic region, for field size 28 x 28 cm^2 and 70 kVp between filter thicknesses of 0.3 and 0.1 mm;

3. In the pelvic region, for field size 22 x 22 cm^2 and 81 kVp between filter thicknesses of 0.3 and 0.2 mm;

The increase factors values in the face and thorax regions are almost identical when those in the pelvic region are smaller, but this difference does not exceed 15% and decreases with decreasing field size.

Fig. 5 shows the results of fitting the straight line to the results obtained for the regions of face, thorax, and pelvis separately. The formulas allow evaluating the increase factors in relation to field size.

Figure 5: Increase factor (D/D10) of the occupational dose rate as a function of field area (S) (radiographic mode).

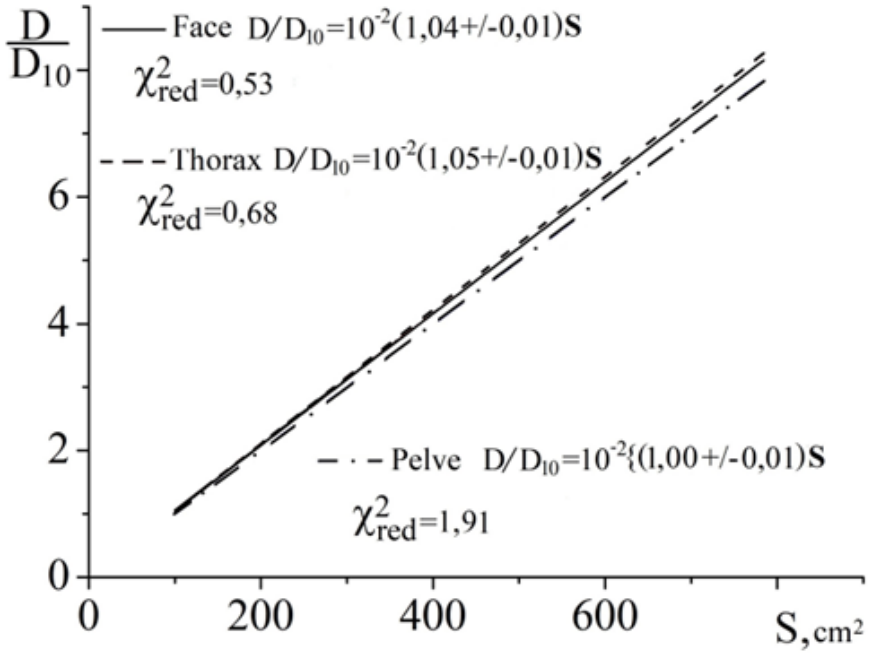

Unlike the dose rate at the exit of the patient's body, in the case of the occupational dose, the dose rate is linearly proportional to the field area. Possible absorption effects of scattered photons do not exceed 1%. Change of scattering angle in this case is very small and it makes no sense to consider it.

3.3. Change in dose rate at the entrance of the patient's body in fluoroscopic mode

Fig. 6 shows the increase factors of the entrance dose rate as a function of field side length for radiographic, fluoroscopic with grade and fluoroscopic without grade modes.

Figure 6: Increase factor (D/D_{12}) of the entrance dose rate as a function of field side length (L) for radiographic, fluoroscopic with grade and fluoroscopic without grade modes.

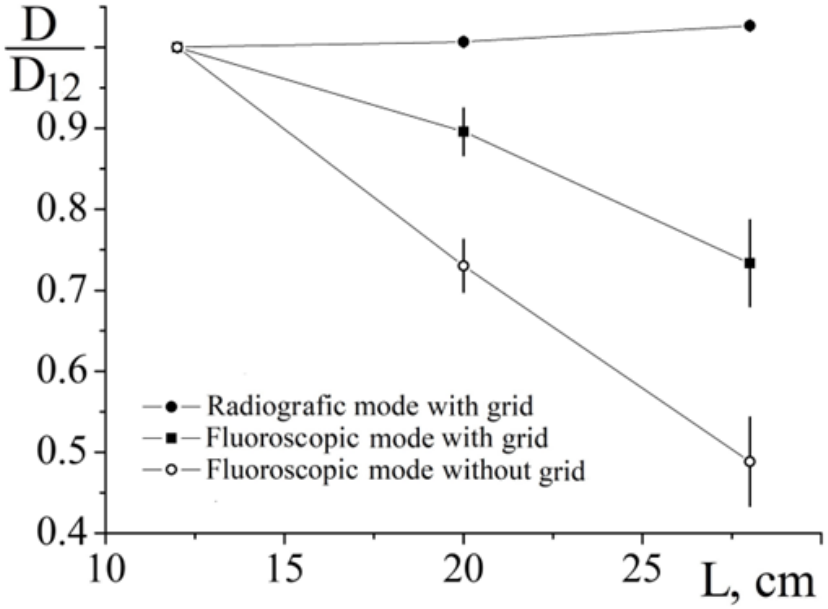

In radiographic mode, where automatic brightness control is not used, the dose rate practically does not change. In fluoroscopic mode, it decreases linearly with the increase of field side length. This effect is almost two times larger without grid and reaches 25% with grid and 50% without grid. To maintain the same brightness with increasing field size, the automatic brightness control has to decrease dose rate at the entrance. In fluoroscopic mode with grade, the part of radiation that was eliminated by grid and that did not reach the detector regulating the activity of the automatic brightness control is not constant. It depends on field size.

Tables 6 and 7 show how the increase factor depends on filtration.

Table 6: Mean values and standard deviations of the increase factor of the entrance dose rate as a function of field size and filter thickness. Fluoroscopic mode with grid.

Field size (cm^2)	Filter thickness, mm			
	0.3	**0.2**	**0.1**	**0**
28 x 28	0.675±0.002	0.722±0.003	0.766±0.003	0.772±0.003
20 x 20	0.867±0.003	0.888±0.003	0.925±0.003	0.904±0.003
12 x 12	1.000±0.004	1.000±0.004	1.000±0.004	1.000±0.004

Table 7: Mean values and standard deviations of the increase factor of the entrance dose rate as a function of field size and filter thickness. Fluoroscopic mode without grid.

Field size (cm^2)	Filter thickness, mm			
	0.3	**0.2**	**0.1**	**0**
28 x 28	0.464±0.002	0.453±0.002	0.482±0.002	0.555±0.002
20 x 20	0.727±0.003	0.693±0.002	0.751±0.003	0.751±0.003
12 x 12	1.000±0.004	1.000±0.004	1.000±0.004	1.000±0.004

As the filter thickness increases, the coefficient decreases, but this effect does not exceed 20%.

The results obtained previously for dose rate at the exit of the patient's body and occupational dose rate in radiographic mode were calculated for the unit of entrance dose rate. It means that before calculating the increase factors, all measured dose rate values were devided by dose rate at the entrance of the patient's body obtained under the same conditions (field size, kVp, filter thickness) to consider possible fluctuations in entrance dose rate (see for exemple Fig. 6). In the case of fluoroscopic mode, if the calculations are also made for the unit of entrance dose, these results do not change. The increase factors of the dose rate at the exit of the patient's body and in the various regions of the professional's body are the same as those in radiographic mode. This is not surprising. Automatic brightness control does not influence the physical processes responsible for these factors (scattering inside the human body). It only changes the dose rate at the entrance.

To understand what happens with the dose rate at the exit of the patient's body and in the various regions of the professional's body considering the effect of the automatic brightness control (not per unit of entrance dose rate), it is necessary to multiply the increase factor obtained for radiographic mode (which increases with field size increase) by the increase factor of the entrance dose rate (which decreases with field size increase in fluoroscopic mode). In fluoroscopic mode the increase of the dose rate at the exit of the patient's body and in the various regions of the professional's body should be less than in

the case of radiographic mode because of the reduction of the entrance dose rate caused by the automatic brightness control.

3.4. Change in occupational dose rate in fluoroscopic mode

The increase factors of the dose rate with automatic brightness control in the various regions of the professional's body are presented in Tables 8-10 as a function of field size and filter thickness for fluoroscopic modes with and without grade.

Table 8: Mean values and standard deviations of the increase factors of the dose rate in the facial region as a function of field size and filter thickness (fluoroscopic mode with and without grid).

Field size (cm^2)	Grid	
	With	**Without**
Filter of 0.3 mm		
28 x 28	4.75±0.25	3.23±0.06
22 x 22	3.63±0.16	2.84±0.29
16 x 16	2.05±0.14	1.84±0.13
10 x 10	1.00±0.08	1.00±0.08
Filter of 0.2 mm		
28 x 28	4.90±0.32	3.54±0.05
22 x 22	3.77±0.35	2.89±0.26
16 x 16	2.05±0.11	1.86±0.10
10 x 10	1.00±0.08	1.00±0.06
Filter of 0.1 mm		
28 x 28	5.05±0.37	3.35±0.16
22 x 22	3.92±0.37	2.98±0.42
16 x 16	2.05±0.08	1.90±0.19
10 x 10	1.00±0.08	1.00±0.04
Without filter		
28 x 28	4.95±0.74	2.93±0.31
22 x 22	3.99±0.39	2.34±0.01
16 x 16	1.95±0.23	1.56±0.14
10 x 10	1.00±0.08	1.00±0.21

Table 9: Mean values and standard deviations of the increase factors of the dose rate in the thorax region as a function of field size and filter thickness (fluoroscopic mode with and without grid).

Field size (cm^2)	Grid	
	With	**Without**
Filter of 0.3 mm		
28 x 28	4.79±0.06	3.17±0.29
22 x 22	3.82±0.15	2.71±0.10
16 x 16	2.18±0.04	1.73±0.10
10 x 10	1.00±0.03	1.00±0.03
Filter of 0.2 mm		
28 x 28	5.11±0.36	3.39±0.08
22 x 22	3.99±0.33	2.74±0.22
16 x 16	2.25±0.04	1.78±0.13
10 x 10	1.00±0.06	1.00±0.04
Filter of 0.1 mm		
28 x 28	5.06±0.26	3.51±0.03
22 x 22	4.09±0.09	2.74±0.29
16 x 16	2.28±0.02	1.69±0.12
10 x 10	1.00±0.08	1.00±0.02
Without filter		
28 x 28	5.31±0.27	3.60±0.32
22 x 22	4.16±0.16	2.83±0.05
16 x 16	2.27±0.09	1.84±0.12
10 x 10	1.00±0.12	1.00±0.06

Table 10: Mean values and standard deviations of the increase factors of the dose rate in the pelvic region as a function of field size and filter thickness (fluoroscopic mode with and without grid).

Field size (cm^2)	Grid	
	With	**Without**
Filter of 0.3 mm		
28 x 28	4.15±0.20	2.63±0.17
22 x 22	3.41±0.22	2.42±0.16
16 x 16	2.01±0.05	1.67±0.05
10 x 10	1.00±0.05	1.00±0.07
Filter of 0.2 mm		
28 x 28	4.52±0.34	2.79±0.23
22 x 22	3.43±0.15	2.67±0.19
16 x 16	2.13±0.08	1.67±0.04
10 x 10	1.00±0.04	1.00±0.09
Filter of 0.1 mm		
28 x 28	4.48±0.26	2.95±0.31
22 x 22	3.60±0.31	2.77±0.21
16 x 16	2.13±0.05	1.69±0.14
10 x 10	1.00±0.06	1.00±0.04
Without filter		
28 x 28	4.55±0.30	3.06±0.34
22 x 22	3.57±0.43	2.72±0.17
16 x 16	2.18±0.08	1.72±0.03
10 x 10	1.00±0.04	1.00±0.09

As was expected, the dose rate growth is significant, but it is lower than that in radiography mode and can reach 500%. As already discussed, such reduction in the increase factor is caused by automatic brightness control that decreases the dose rate at the body entrance with increasing field size. The effect of filter thickness was not observed.

Fig. 7 shows the increase factor of the occupational dose rate as a function of field side length and area in fluoroscopic mode with and without grid. The curves shown are the results of fitting the second-order polynomial to the results obtained for the regions of face,

thorax, and pelvis separately. The formulas allow evaluating the increase factors in relation to the field size.

Figure 7: Increase factor (D/D_{10}) of the occupational dose rate as a function of field side length (L) and area (S) (fluoroscopic mode).

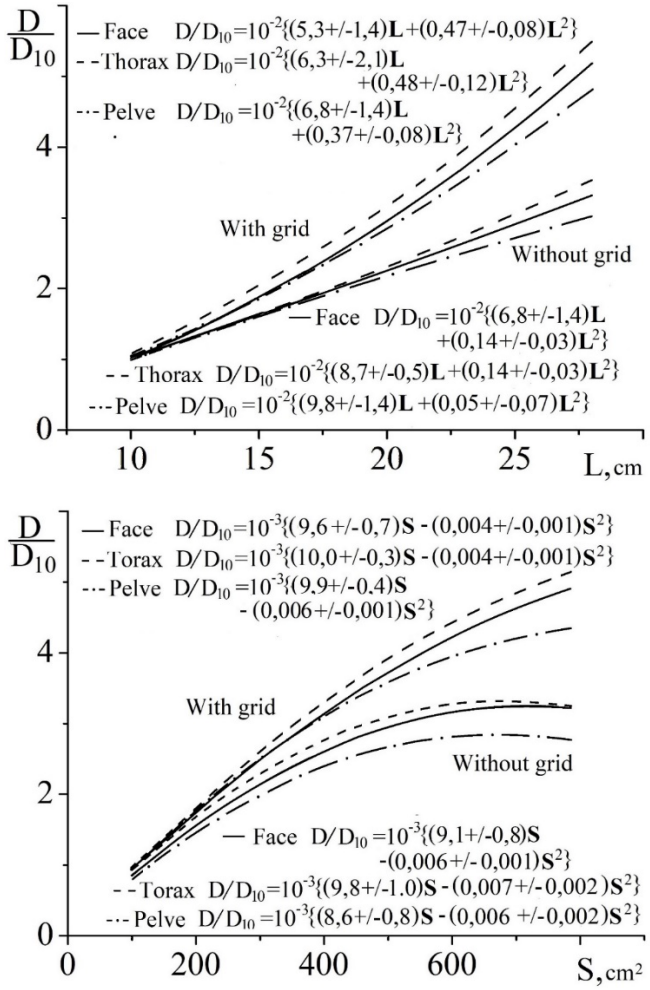

The lines in Fig. 7 give the impression that the occupational dose rate is highest for thorax and lowest for pelvis. However, analysing the errors of the fitting coefficients in Fig. 7, it is clear that this difference was not statistically confirmed. Because of the automatic brightness control, the increase of the dose rate with increasing field size is slower than in the case of radiography mode.

4. CONCLUSIONS

In the present work, we studied how expansion of the irradiation field size influences dose rate to patient and staff in fluoroscopy and radiography for different primary X-ray spectra. It was observed that:

- In radiographic mode, dose rate at the exit of the patient's body increases with the increase of field size. This increase reaches 85% and its dependence on primary X-ray spectrum does not exceed 4%. The number of scattering points that contribute to the increase factor is linearly proportional to the field area, but the dose rate increases much more slowly.
- The increase of occupational dose rate in radiographic mode reaches 850% and is linearly proportional to the field area with the precision better than 1%.
- In fluoroscopic mode, dose rate at the entrance of the patient's body decreases proportionally to the increase of field side length because of the automatic brightness control. This effect reaches 25% with grid and 50% without grid.

ACKNOWLEDGMENT

This study was partially funded by Coordenação de Aperfeiçoamento de Pessoal de Nível Superior - Brasil (CAPES) - Finance Code 001, Conselho Nacional de Desenvolvimento Científico e Tecnológico (CNPq), Comissão de Energia Nuclear (CNEN) and Fundação Araucária de Apoio ao Desenvolvimento Científico e Tecnológico do Paraná (FA).

CONFLICT OF INTEREST

All authors declare that they have no conflicts of interest.

REFERENCES

[1] EUROPEAN COMMISSION. European Guidelines on Quality Criteria for Diagnostic Radiographic Images in Paediatrics. **EUR 16261**, ECSC-EC-EAEC, Brussels, Luxembourg, 1996. Available at: https://op.europa.eu/en/publication-detail/-/publication/47eb62b0-698d-4166-bc34-cc3f8d07d2e3

[2] EUROPEAN COMMISSION. European Guidelines on Diagnostic Reference Levels for Paediatric Imaging. **Radiation Protection N°185**, Luxembourg: Publications Office of the European Union, 2018. Available at: https://op.europa.eu/en/publication-detail/-/publication/6e473ff5-bd4b-11e8-99ee-01aa75ed71a1/language-en

[3] International Atomic Energy Agency. Patient Dose Optimization in Fluoroscopically Guided Interventional Procedures. **IAEA-TECDOC-1641**, IAEA, Vienna, 2010. Available at: https://www.iaea.org/publications/8176/patient-dose-optimization-in-fluoroscopically-guided-interventional-procedures

[4] International Commission on Radiological Protection. Radiological protection in cardiology. **ICRP Publication 120. Ann. ICRP**, v. 42, n. 1, 2013. Available at: https://www.icrp.org/publication.asp?id=ICRP%20Publication%20120

[5] International Commission on Radiological Protection. Radiological protection in paediatric diagnostic and interventional radiology. **ICRP Publication 121. Ann. ICRP**, v. 42, n. 2, 2013. Available at: https://www.icrp.org/publication.asp?id=ICRP%20Publication%20121

[6] International Commission on Radiological Protection. Diagnostic reference levels in medical imaging. **ICRP Publication 135. Ann. ICRP**, v. 46, n. 1, 2017. Available at: https://www.icrp.org/publication.asp?id=ICRP%20Publication%20135

[7] United Nations Scientific Committee on the Effects of Atomic Radiation. Sources, Effects and Risks of Ionizing Radiation. **UNSCEAR 2020/2021 Report**, United Nations, New York, 2022. Available at: https://www.unscear.org/unscear/en/publications/2020_2021_1.html

[8] QUINN B. CARROLL. **Radiography in the digital age: Physics Exposure Radiation Biology.** 2600 South First Street, Springfield, Illinois 62704: Charles C Thomas Publisher, LTD, 2018. ISBN 978-0-398-09215-3.

[9] NUNES, G. S.; JAKUBIAK, R.R.; DORO, R.B.; SETTI, J.A.P.; DENYAK, V. Occupational Dose in Pediatric Seriography of the Esophagus, Stomach and

Duodene. **Rev. Bras. Fís. Méd.**, v. 16:572, p. 1-5, 2022. Available at: https://www.rbfm.org.br/rbfm/article/view/572/599

[10] NUNES, G. S.; DORO, R.B.; JAKUBIAK, R.R.; SETTI, J.A.P.; BARROS, F.S.; DENYAK, V. Occupational Dose in Pediatric Barium Meal Examinations, **IFMBE Proceedings**, v. 83, p. 1051-1054, 2022. Available at: https://link.springer.com/chapter/10.1007/978-3-030-70601-2_156

[11] RaySafe. RaySafe X2 Specifications. Disponível em: https://www.raysafe.com/sites/default/files/2021-07/raysafe_x2_specification_brochure.pdf. Acesso em: 27 mar. 2023.

[12] Agência Nacional de Vigilância Sanitária. **Radiodiagnóstico Médico: Desempenho de Equipamentos e Segurança.** Brasilia, Editora Anvisa, 2005. p. 1-104.

[13] PORTO, L.; LUNELLI, N.; PASCHUK, S.; OLIVEIRA, FERREIRA, J.L.; SCHELIN, H.; MIGUEL, C.; DENYAK, V.; KMIECIK, C.; TILLY, J.; KHOURY, H.; Evaluation of entrance surface air kerma in pediatric chest radiography, **Rad. Phys. Chem.**, v. 104, p. 252-259, 2014. Available at: https://www.sciencedirect.com/science/article/abs/pii/S0969806X14000590

LICENSE